CHAPTER

1

Structure from motion photogrammetric technique

Anette Eltner[a], *Giulia Sofia*[b]

[a]Institute of Photogrammetry and Remote Sensing, Technische Universität Dresden, Dresden, Germany [b]Department of Civil and Environmental Engineering, University of Connecticut, Storrs, CT, United States

OUTLINE

1 Introduction

Structure from motion (SfM) photogrammetry provides hyper-scale three-dimensional (3D) landform models using overlapping images acquired from different perspectives with standard compact cameras (including smartphone cameras) and geo-referencing information. As applied to the remote sensing of geomorphology, it is not so much a single technique,

https://doi.org/10.1016/B978-0-444-64177-9.00001-1

but rather a workflow employing multiple algorithms developed from computer vision, traditional photogrammetry, and more conventional survey techniques (Carrivick et al., 2016). Recent literature has provided reviews on the importance of SfM in geosciences (Carrivick et al., 2016; Eltner et al., 2016; Smith et al., 2016) or specific scientific contexts (Mancini et al., 2013; Dietrich, 2016; Entwistle et al., 2018). This contribution builds on the existing literature, to provide a showcase of the technology, relevant to the remote sensing of geomorphology.

1.1 Brief historical summary and state of the art

The roots of SfM lie in two key fields: photogrammetry and computer vision. When techniques from these fields are combined with both automation and precision, the result is a comprehensive tool (Pierrot-Deseilligny and Clery, 2011) for geomorphological applications. Photogrammetry is a relatively old technique (Slama et al., 1980). In this field, the reconstruction efforts of pioneers in the 1840s initially attempted using a pair of ground cameras separated by a fixed baseline and followed by applications using cameras for estimating the shape of the terrain from ground and aerial photographs (Maybank, 1993). With the introduction of aeroplanes and space photography, the development of photogrammetry flourished, with 2D photographs used to rectify images into appropriate coordinates, or mosaicking multiple frames to estimate structures or ground elevation. In a parallel effort, the computer vision community provided the first early algorithms for 3D scene reconstructions by stereo images (Marr and Poggio, 1976) or to pioneer work on motion-based reconstruction (Ullman, 1979).

The prime formalisms derived in these two communities provided the most important foundational theory for the SfM community. However, advances in SfM have been spurred mostly due to the wide range of modern applications. A search in the academic publications database Web of Sciences (WoS) for Structure from Motion (made in August 2018) delivered >3000 records since the early 1980s (Fig. 1), covering as many as 125 fields of study.

Computer science and artificial intelligence is the category with the most counts of that phrase. Engineering is ranked second, remote sensing is fourth, and geosciences is currently ranked sixth. This wide range of applications of SfM results in research with different goals, hence emphasizing multiple ways of addressing SfM problems in space and time. The computer vision field features much older publications than other fields, with the first papers published in the 1980s (Bolles et al., 1987) introducing a technique for building a 3D description of a static scene from a dense sequence of images, and the latest (Zhu et al., 2018) discussing new methods for bundle adjustment (the optimization method needed to simultaneously retrieve the image pose parameters from overlapping images considering corresponding image points). Notably, the geosciences have only started producing publications incorporating SfM photogrammetry in the past decade, but with improvements in the technique moving at an incredible speed: note that a similar search in 2015 by Carrivick et al. (2016) ranked Geosciences in the ninth position. In this field, the first work was published (according to WoS) by Heimsath and Farid (2002). Here, results from three unconstrained photographs characterized hillslope topography, and yield to an estimated surface with errors of the order of 1 m. In comparison, one of the last papers published in the field at the time of the search (Smith and Warburton, 2018) illustrates that topographic data from SfM photogrammetry (with errors on the scale

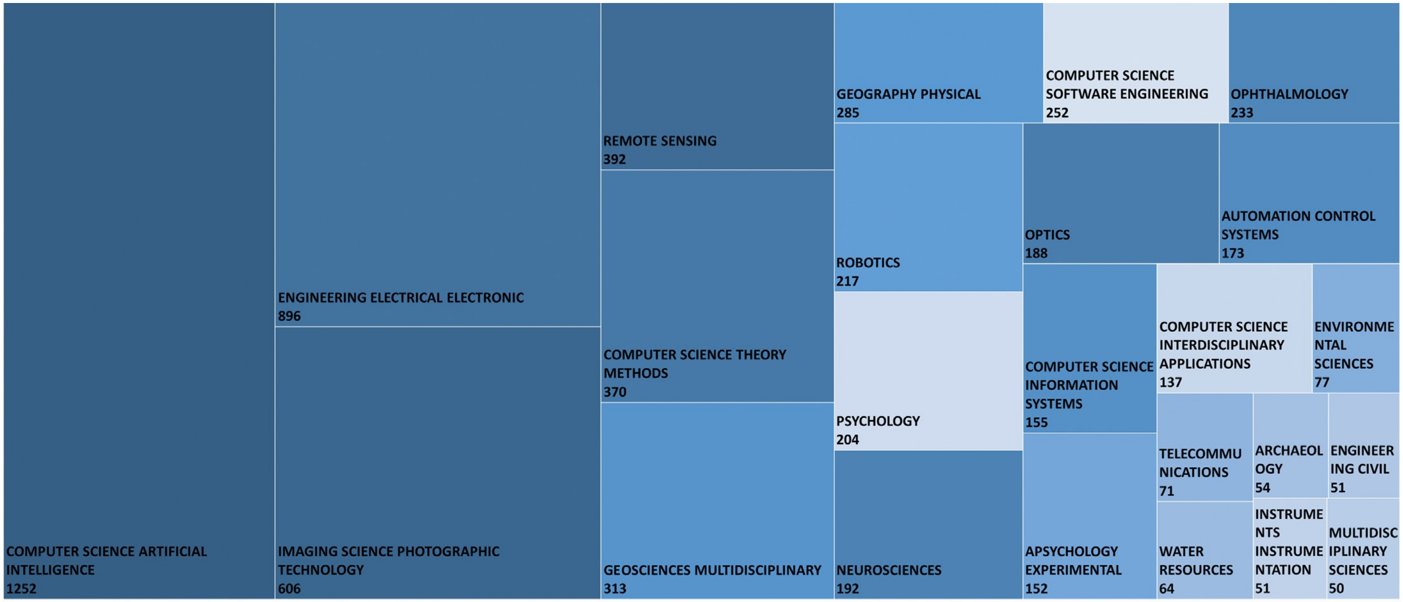

FIG. 1 "Structure from motion" search in academic databases: first 25 results and number of records per discipline (as of August 2018).

of <1 mm) inherits enough information to analyze the relationship between geomorphological process and form, at the microscale (few millimeters).

These few examples show an evolution of SfM photogrammetry in time and topics. In the computer vision field, the emphasis remains on methods for obtaining information from images, whereas the evolution of SfM photogrammetry is different in geosciences. Early SfM photogrammetry studies in geosciences emphasized the accuracy of reconstruction, whereas modern geosciences applications focus more on the information that can be retrieved from such analyses.

1.2 Reasons for success in geomorphological surveys

For geomorphological studies, the availability of a high-resolution topographic dataset is fundamental, particularly so for those systems characterized by a complex morphology. We find four main reasons for the success of SfM photogrammetry in geomorphology: (i) spatial accuracy and temporal frequency, (ii) cost; (iii) speed and ease of use. A further reason for SfM's success, although it is still in its exploratory phase, is and (iv) the possibility of involving citizens in science. These points are intrinsically interrelated and build on each other to determine the success of the technique in geosciences.

In geosciences, SfM photogrammetry is a workflow that is virtually independent of spatial scale (Carrivick et al., 2016), it allows potentially unlimited temporal frequency (Carrivick et al., 2016) and can provide point-cloud data comparable in density and accuracy to those generated by terrestrial and airborne laser scanning at a fraction of the cost (Westoby et al., 2012). It offers therefore exciting opportunities to characterize surface topography in unprecedented detail, allowing workers to detect elevation, position, and volumetric or areal changes that are symptomatic of earth surface processes across spatial (see Section 3) and temporal (see Section 4) scales.

When speaking about the costs of a SfM photogrammetry application, they can vary depending on sensors, survey design, and ground control points (GCPs)—when present. SfM photogrammetry sensors are based on consumer-grade cameras, or even smartphones (Micheletti et al., 2014; Prosdocimi et al., 2016; Sofia et al., 2017), which can be handheld or mounted on UAV systems. The sensors, mounting systems or cameras can vary substantially in price and complexity, but the trade-offs between these and the quality of the resulting data are not well constrained (Cook, 2017). In general, however, the availability of these sensors, and the opportunity of applying SfM photogrammetry to satellite images (Sofia et al., 2016), historical photographs or opportunistic sensors (see Sections 4.1 and 4.2), has drastically reduced the costs of surveys with respect to airborne or terrestrial laser scanners or GNSS. Geo-referencing forms a fundamental part of topographic surveys and, for SfM photogrammetry work, dense deployments of carefully measured GCPs are usually used, which can represent a substantial proportion of the overall survey effort (James et al., 2017a). However, new applications are also evaluating the opportunity of directly referenced surveys (see Section 2.3).

The availability of free or low-cost fully automated photogrammetric software, of cameras of any level (from reflex to smartphones), and the recent increase of drones also in the private and public sectors (News organizations, journalists, and private citizens have employed UAVs to provide glimpses of natural disaster, for example), allows just about anyone to generate 3D models for various purposes (Remondino et al., 2017). Processing of the data, in fact, does not necessarily need proprietary software, e.g., (AgiSoft, 2010), but numerous open-source photogrammetric (OSP) software, e.g., OpenMVG (https://github.com/openMVG/openMVG), OpenDroneMap (https://github.com/OpenDroneMap), MicMac (http://logiciels.ign.fr/?Micmac), VisualSFM (Wu, 2011, 2013), SF3M (Castillo et al., 2015), and 3D data processing tools, e.g., CloudCompare (Girardeau-Montaut, 2015) or MeshLab (Cignoni et al., 2008) among others, are emerging.

Geographic research is nowadays a data-rich environment, where the most recent advance is not just the resolution of the data, but the variety and the rapidity with which we can capture georeferenced data (Miller and Goodchild, 2015). Citizen science can improve research, but it suffers from necessitating specialized training and simplified methodologies that reduce research output (Raoult et al., 2016). The ease of the use of SfM photogrammetry with a range of sensors can enable the opportunity of participatory and opportunistic crowdsourced sensing, facilitating the involvement of crowd communication. It is important to underline, however, that this comes to a hidden cost: the majorities of image-based users are often unaware of strengths and weaknesses of the used methodology and software, employing it much like a black-box where they can drop photographs in one end and retrieve a (hopefully) completed 3D model on the other end. It is fundamental, therefore, to provide geospatial tools integrated with appropriately designed instructional materials (Sofia et al., 2017).

2 Method

The workflow of SfM photogrammetry can be put in a nutshell as follows (e.g., James and Robson, 2012; Smith and Vericat, 2015; Eltner et al., 2016; Schonberger and Frahm, 2016): In the first step features are detected in each image and matched between overlapping frames (e.g., using the SIFT algorithm from Lowe, 2004). These homologous image points are used in a second step to reconstruct the image network geometry in an iterative bundle adjustment (e.g., Snavely et al., 2006). During this phase, intrinsic camera parameters, describing the interior camera geometry (focal length and principle point plus additional distortion parameters), and extrinsic parameters, describing the position (three shifts) and orientation (three rotations) at which images have been captured, are estimated. Furthermore, 3D object coordinates in an arbitrary coordinate system are calculated from the 2D image coordinates of the homologous image points, creating a sparse point cloud. With the knowledge about the image network geometry, it is possible to retrieve a dense point cloud, which comprises the calculation of a corresponding 3D point for almost each image pixel. For a summary of dense matching algorithms, we refer to Remondino et al. (2014). The resulting 3D point cloud can be geo-referenced during the adjustment, and the additional information can be considered to optimize intrinsic and extrinsic camera parameters, or afterwards with a similarity transformation, thus having no further potential for improvement of the adjustment.

Although algorithmic advances and software tools make the application of SfM photogrammetry simple in its usage for topographic reconstruction, basic knowledge about photogrammetric principles are still required for a robust accuracy assessment (e.g., Carbonneau and Dietrich, 2017) to avoid potential bias in the 3D model leading to misinterpretation of geomorphological forms and processes. The increased awareness in this regard is highlighted by increased interest in proper parameter settings and their effect on the final model as illustrated in the next section.

2.1 Choosing suitable settings to comply with the application at hand

Various influences occur on the quality of the final 3D reconstructed surface model using SfM photogrammetry (James et al., 2019). Careful considerations are necessary during both data acquisition and processing. Different impacts on model quality, trade-offs, and guidelines to achieve most suitable surface models in geo-scientific applications are discussed in detail by Eltner et al. (2016) and Smith et al. (2016). Thus, this section builds on those reviews, and summarizes in detail key elements and the related recent literature, providing suggestions to improve SfM photogrammetry models.

2.1.1 Image quality

Image quality is considered to be of great importance because SfM photogrammetry relies on the successful detection and matching of image features, which is one of the main tasks of photogrammetry (Gruen, 2012). Because image quality significantly influences these first steps, making sharp and well-exposed images are the basis for accurate further data processing (O'Connor et al., 2017). Thus, in order to obtain reliable 3D models, it is important to start by choosing the right camera and the most suitable configuration for optimized image capture (Mosbrucker et al., 2017). It is important to note that each parameter setting can improve image quality, and the optimal choice is a trade-off between camera settings that consider the application at hand (Mosbrucker et al., 2017; O'Connor et al., 2017). The main points for an optimal image quality (highlighted by Mosbrucker et al., 2017 and O'Connor et al., 2017) are summarized here:

- Images should be captured in RAW format rather than JPEG, due to significantly higher bit-depth, e.g., 12–16-bit vs 8-bit image information, respectively.
- Cameras with larger sensors should be favored because they enable a higher signal to noise ratio, as pixels are generally larger and thus more light can be captured.
- The dynamic range of the camera is the camera's ability to resolve the brightest (saturation level) and darkest (minimum level of detection) signals, which depends on the resolution of the analogue to digital signal converter. This range should be set as high as possible, to allow to capture the entire range of luminance of an observed scene.
- Regarding lenses, a good trade-off between overlap and distortion effects has to be chosen. For instance, wider angled lenses allow for higher image overlap, but mostly also depict higher radial distortions.
- For close-range applications, depth-of-field has to be considered, and therefore aperture should be chosen correspondingly.
- Furthermore, exposure settings are important, which can be evaluated using the exposure triangle with ISO, aperture and shutter speed at each corner. ISO should be chosen as low as possible because less noise and a higher dynamic range are the consequences. Shutter speed should also be as low as possible to avoid blur due to motion but still receive enough light at the sensor. These settings change with different lenses, object distances, and moving objects.
- Finally, it should be noted that images with high quality are also achievable with compact cameras if fixed lenses and large sensors are considered, which is important considering pay-load aspects in UAV applications.

A detailed description of the data and its processing enables a comprehensive assessment of 3D model retrieval. Thus, for better evaluation and comparability of image quality, data including metadata about settings during image acquisition should be made available in an open access repository (O'Connor et al., 2017). This could complement the documentation spreadsheet introduced by Eltner et al. (2016) that aims to record data-acquisition settings during the field campaigns and parameter setting during subsequent data processing.

2.1.2 Ground sampling distance

The distance between the camera and the area of interest influences the accuracy and resolution of the reconstructed surface model, revealing an inverse relationship between distance and model accuracy (Smith and Vericat, 2015; Eltner et al., 2016). However, instead of referring to this distance value alone, Mosbrucker et al. (2017) suggest also considering ground sampling distance (GSD), which describes the ratio between the distance in image space to the distance in object space. Different cameras with different focal length and different sensors (and thus pixel pitch) lead to different GSDs, even when objects are captured from the same distance.

2.1.3 Image network geometry

The orientation and position from which images are taken is a key aspect of a reliable 3D reconstruction. Images should have a high overlap from different perspectives. The distances between images (which is called the base) should be big enough to avoid glancing ray intersections due to very small parallax angles. At the same time, images should not be taken too far apart to avoid changes in the image content appearance so great that no homologous points are detected. Each point for which a 3D model is to be retrieved should be seen in at least three images. The more images the better due to increasing redundancy in image measurements. Furthermore, the image network geometry should comprise convergent images, if possible, to avoid systematic errors such as domes (James and Robson, 2014). Other advice regarding an ideal geometry to avoid unfavorable error propagation include capturing the area of interest from different distances (Micheletti et al., 2014) and cross-flight stripes in the case of UAV imagery (Gerke and Przybilla, 2016).

2.1.4 Camera parameter choice during bundle adjustment

Deciding which parameters are to be considered during bundle adjustment, and with what weights, is essential for a robust model reconstruction from overlapping images. James et al. (2017a) demonstrated that estimating too many camera model parameters during bundle adjustment can lead to over-parameterization and thus errors in the final model. For instance, in many applications, two radial distortion parameters are sufficient although more values could be implemented. Remondino et al. (2012) previously discussed the relevance of choosing the correct number of parameters. They observed dome effects for SfM software tools that estimated the interior camera geometry for each image and suggested using only one interior camera model if one camera has been utilized to capture the images. Similar conclusions were also supported by Rosnell and Honkavaara (2012). A potential approach to check for over-parameterization is to consult correlation values between estimated camera parameters: they should be low. Furthermore, the significance of each estimated parameter can be consulted to check for over-fitting (James et al., 2017b).

2.1.5 Referencing: GCP weights and distribution

The precision and distribution of referencing and control data, i.e., ground control points (GCPs) and checkpoints (CPs, that are GCPs not implemented during the bundle adjustment), respectively, are important to guarantee and control the quality of the final scaled model. The weights of the precision of image measurements of GCPs and tie points have to be chosen accordingly, to avoid model errors due to over-fitting at the GCPs. Furthermore, reprojection errors at the CPs should not be much higher than at the GCPs (James et al., 2017a).

Generally, GCPs should be surrounding the area of interest. Also, they need to be well distributed. A minimum of four GCPs is necessary for increased accuracies, with errors in height increasing with increasing distance to GCPs (Tonkin and Midgley, 2016). Recent advances in direct geo-referencing, where models are referenced directly considering the orientation and position from which cameras were triggered, indicate that GCPs might become less important in future applications in geomorphology (see Section 2.3).

2.1.6 Exterior influences

Surface properties, e.g., texture, and illumination conditions influence feature detection and matching significantly. Overcast conditions are preferred to strong shadows. Regarding surface properties, on the one hand, surface texture has to be sufficient, e.g., snow is less suitable due to potentially missing contrast, but on the other hand, it should not be too complex, e.g., vegetation, whose appearance changes distinctively within shortest distances and minimal changes of perspectives. Recent studies, however, have shown that it is possible to reconstruct single blades of grass if the number of images is high enough (Kröhnert et al., 2018).

2.2 Accuracy considerations in geomorphological applications

Due to the many parameters that influence the accuracy of the final 3D model derived from the SfM-photogrammetry approach, error reliability is not as high as, for instance, point clouds derived from terrestrial laser scanning (TLS). Therefore, the need for robust error modeling is important when using SfM photogrammetry, especially considering the variety of applications in geomorphology at varying spatiotemporal scales. When performing error modeling, distinctions should be made between error reproducibility, i.e., error behavior under different conditions, and error repeatability, i.e., error behavior under the same conditions (Goetz et al., 2018). Furthermore, it is important to distinguish between constraining 3D accuracies due to internal and external causes (James et al., 2017b). Internal precision is influenced by image network geometry and tie-point measurements, whereas external precision relies on actual geo-referencing. Recent studies have focused on modeling of error behavior of SfM-photogrammetry data to improve data quality in geomorphic studies (James et al., 2017a,b; Wasklewicz et al., 2017).

SfM photogrammetry is not as rigorous in regards to the precision weights when compared to traditional photogrammetry, and therefore improvements to the accuracy of the final SfM-DEM (digital elevation model) are still possible if photogrammetric principles beneath SfM photogrammetry are considered (James et al., 2017a). James et al. (2017a) provide a workflow to consider and minimize errors when using SfM photogrammetry, which they illustrate with significantly improved error to distance ratios for two case studies. Thereby, the weight consideration of reference accuracy of GCPs in object space, as well as image measurement accuracy of tie points and GCPs in image space are important to avoid falsely fitting during bundle adjustment (James et al., 2017a).

Errors are spatially highly correlated when using SfM photogrammetry (James et al., 2017b), which is in contrast to other high-resolution topography methods such as TLS, where spatially independent, error behavior is assumed (e.g., Abellán et al., 2009; Kromer et al., 2015). Thus, rather than using one level of detection (LoD) applied to the entire DEM of difference for multitemporal change detection, consideration of spatial correlation is important (James et al., 2017b). James et al. (2017b) use Monte Carlo simulation to calculate precision maps, which they combined with an adopted M3C2 algorithm, which already considers a variable LoD depending on the complexity of the terrain (Lague et al., 2013) to estimate a spatially correlated error of the SfM-photogrammetry point cloud. However, it should be noted that precision maps are not able to detect systematic errors such as domes (e.g., Eltner and Schneider, 2015) and thus independent reference data, e.g., CPs, are needed for a robust accuracy estimation (James et al., 2017b).

2.3 Direct geo-referencing (DG) for flexible UAV applications

Recent advances in the field of devices, combined with advances in the retrieval of accurate sensor orientation and position of the camera during image acquisition, have the potential to enable SfM-photogrammetry applications based on UAV imagery that does not require GCPs. This could potentially revolutionize collection of SfM-photogrammetry data in remote or dangerous areas, or areas under very frequent observation. Here we discuss the potential for direct geo-referencing (DG) for aerial platforms.

Benassi et al. (2017) divided geo-referencing into indirect sensor orientation (InSO), direct sensor orientation (DSO), and integrated sensor orientation (ISO). InSO, or indirect geo-referencing (IG), uses tie points, GCPs and bundle adjustment to reference the data, and potentiality also considers camera self-calibration. DSO uses solely camera orientation/position estimates, which complicates reliable camera self-calibration, resulting in potential systematic errors due to unresolved image block deformations. ISO considers camera position and orientation as well as tie-points to perform bundle adjustment. Furthermore, a few GCPs might be considered when using ISO, which can be important if self-calibration is also performed. In this study, we refer to DG as a method that incorporates both DSO and ISO. In general, DG refers to the direct implementation of estimated orientation and position information of the central projection center of the camera during image capturing to reference image-based reconstruction products (Pfeifer et al., 2012).

Utilizing UAV data with DG has great advantages because access to changing or dangerous environments for the purpose of including GCPs will not be needed. Inclusion of GCPs is still one of the main limitations for flexible UAV applications (e.g., Carbonneau and Dietrich, 2017; Forlani et al., 2018). Furthermore, IG implies high demands regarding the GCP distribution (e.g., James et al., 2017a; Tonkin and Midgley, 2016), because low-cost position and orientation estimation devices, as well as low-cost cameras, demand robust GCP networks for reliable adjustment during 3D reconstruction (Gerke and Przybilla, 2016).

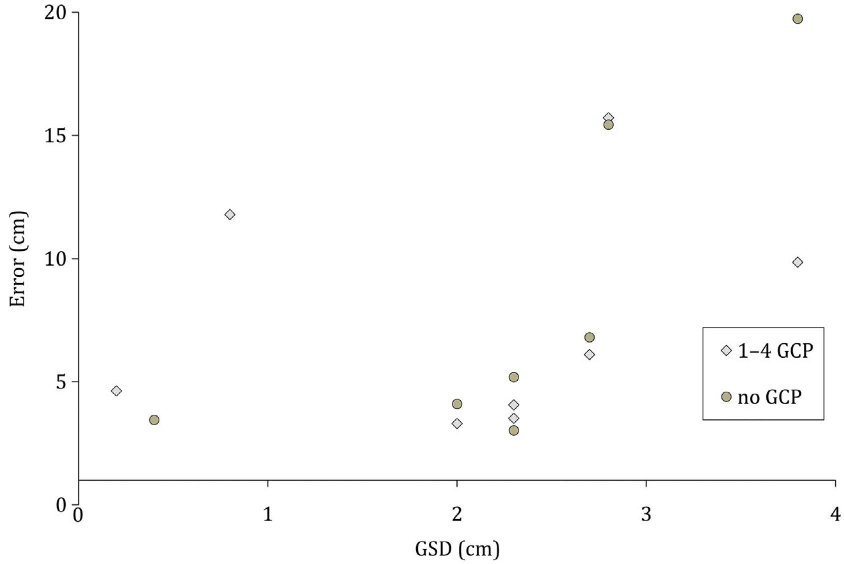

FIG. 2 Error estimates (standard deviation or RMSE) of case studies using direct geo-referencing or integrated sensor orientation (considering 1 to a maximum of 4 GCPs) are related to round sampling distance (GSD) considering case studies by Rehak et al. (2013); Stöcker et al. (2017); Eling et al. (2015); Mian et al. (2015); Rehak and Skaloud (2016); Forlani et al. (2018); Benassi et al. (2017); Gabrlik et al. (2018); and Gerke and Przybilla (2016). If GCP and no GCP were evaluated within one study, solely, the case for GCP included is illustrated.

Most current low-cost UAVs are equipped with GNSS devices that do not enable real-time kinematic processing (RTK) or postprocessing kinematic (PPK) to correct the GNSS signal leading to accuracies of the final 3D model in meter-ranges (Turner et al., 2014) or dm-ranges (Gerke and Przybilla, 2016; Hugenholtz et al., 2016; Stöcker et al., 2017). However, if RTK- or PPK-GNSS is possible, this will result in a high potential for DG of UAV data (Bláha et al., 2012) and cm-ranges can be achieved (Fig. 2). Furthermore, using RTK- or PPK-GNSS can help to decrease image block deformations significantly (Gerke and Przybilla, 2016), and thus systematic errors such as domes in the 3D model (James et al., 2017b) might be mitigated. Generally, an integrated GNSS and IMU (inertial measurement unit capturing angular changes and accelerations) approach is used in support of DG to allow for precise flight-trajectory reconstruction. This provides knowledge about the position, attitude, and velocity of the UAV during image capturing (Chiang et al., 2012; Pfeifer et al., 2012; Eling et al., 2015). Due to the weight constraints of UAVs, microelectromechanical systems (MEMS) are utilized as low-cost IMUs (Pfeifer et al., 2012).

2.3.1 Achievable accuracies

Errors of the SfM-photogrammetry result reach about 0.1% of flying height for low-cost GNSS devices with no kinematic processing (Carbonneau and Dietrich, 2017). However, the picture is different for RTK- or PPK-GNSS applications. To evaluate the accuracies of the final 3D model, studies using DG with RTK- or PPK-GNSS have been compared. It has to be noted that different studies utilize different parameters, e.g., some use lever arm and boresight corrections and others do not consider their influence. Error ranges are high, i.e., between 2 and 20 cm, and errors increase with increasing GSD (Fig. 2).

Furthermore, these studies reveal that error improves significantly if camera calibration is performed with self-calibration instead of a pre-/postcalibration (e.g., from 55.3 to 4.1 cm in Gabrlik et al., 2018). Also, GCP consideration is important because the studies show that if at least one GCP can be implemented, the error decreases strongly (e.g., from 10 to 3 cm in Forlani et al., 2018). Beside absolute error, relative error (ratio between measured error and object distance, Eltner et al., 2016) is diverse for all studies, as well. Average ratio amounts are 1:1300 with a standard deviation of 700.

2.3.2 Guidelines for DG applications

If direct DG is performed, several aspects have to be accounted for:

– Pre- or postflight camera calibration should be considered if no GCPs are possible because residuals of the self-calibration of the interior camera geometry propagates into the final 3D model in object space, which can be compensated for by exterior orientation when GCPs are used in the bundle block adjustment (Gerke and Przybilla, 2016; Forlani et al., 2018). Also, systematic errors are absorbed by exterior camera orientations and positions and thus estimated positions and orientations do not coincide anymore with actual physical image network geometry during image capturing, which, however, does not matter if the focus is on the final accuracy of object points (Cramer et al., 2000).
– If possible, at least one GCP should be included, which is relevant for estimating interior camera geometry during self-calibration, allowing for almost identical results to IG applications (Benassi et al., 2017; Forlani et al., 2018; Gabrlik et al., 2018). Using many more GCPs compared to just one indicates no further improvement of the final 3D model (Gerke and Przybilla, 2016).
– Specific flight patterns should be chosen, especially if camera self-calibration is aimed for, to avoid unfavorable parameter correlation, i.e., use cross-flights, especially if the terrain comprises no large height shifts (Gerke and Przybilla, 2016), fly at different heights, and/or capture convergent images (James et al., 2017a).
– The importance of weights given to the parameters of exterior orientation has to be considered. Orientation estimates of the sensor are still not sufficient for high weights on angles and hence achieve best results if high weights are assigned to the position but low weights on attitude during bundle adjustment (Stöcker et al., 2017). Furthermore, the choice of a set of parameters has an impact on height accuracy, and using the parameter weights can lead to different accuracies with different software, potentially due to different consideration of weights of observations (Benassi et al., 2017).
– Offsets between projection center of the camera and the position of the GNSS receiver [i.e., lever arm, and orientation of the IMU, i.e., boresight (angular misalignments)] need to be estimated (Chiang et al., 2012). Furthermore, synchronization issues between the camera shutter release and GNSS/IMU signal logging have to be considered (Gabrlik et al., 2018).

Ultimately, the best practice for flexible and accurate direct referencing of UAV data is the combination of traditional aerial triangulation and implementation of directly measured, sensor-position information. Thereby for highest accuracies, position estimates are used as approximation values during adjustment, in combination with tie points and very few GCPs, if the terrain allows for it (Chiang et al., 2012). Estimates of camera position mitigate block deformation issues (Gerke and Przybilla, 2016) and support tie-point detection in areas of unfavorable texture (Stöcker et al., 2017), whereas GCPs can be further used as checkpoints to enable reliable error estimates.

3 Reconstructing processes across space

Accurate, precise, and rapid acquisition of topographic data is fundamental to many subdisciplines of physical geography (Smith et al., 2016). Conceptually, the patterns of earth surface processes detected in any topographic dataset are a function of scale. The scale of a study can relate to the overall area encompassed by an investigation (extent) or the size of the individual units of observation (process resolution, which we define as *grain*). In SfM-photogrammetry applications in geomorphology, several fundamentally different extents and grains concerning processes are known, but the boundaries or thresholds among them may be fuzzy.

At the smaller grain, for example, the rigorous modeling and quantification of soil-water erosion processes require detailed information about the topography of the land surface with appropriate resolution and accuracy. Thanks to SfM photogrammetry, this microscale grain can be assessed at multiple extents (hillslope, plot, and micro-plot scale; see Fig. 3), allowing quantification of detailed physical changes of soils and their influence on surface morphology even at submillimeter resolution (Kaiser et al., 2018). Among the challenges of SfM photogrammetry in this type of analyses, we can mention the establishment of a common and sufficient reference system for the different DEMs considered, determination of errors in the generation of DEMs, selection of appropriate criteria to obtain reliable changes, error propagation, and validation of the procedure by comparing the results with actual sediments collected during the experiment (Gessesse et al., 2010; Hänsel et al., 2016; Glendell et al., 2017; Prosdocimi et al., 2017; Balaguer-Puig et al., 2017a,b; Eltner et al., 2018; Tarolli et al., 2019). A further problem is that many geoscience processes associated with soil surface microtopography occur on naturally vegetated surfaces, but few guidelines exist for the acquisition and treatment of SfM photogrammetry data on vegetated surfaces (Nouwakpo et al., 2015).

Increasing the grain, remote sensing in fluvial geomorphology using SfM photogrammetry has increased significantly in last 5 years (Entwistle et al., 2018), with many recent advances in, for example, river restoration (Marteau et al., 2017; Woodget and Austrums, 2017). From the smallest to the largest scale, SfM photogrammetry has been proven useful in laboratory flumes (Morgan et al., 2017), for grain size measurements (Micheletti et al., 2014; Bertin and Friedrich, 2016; Pearson et al., 2017), for erosion assessment (Prosdocimi et al., 2016; Hemmelder et al., 2018; Jugie et al., 2018) or river ice quantification at embankment level (Alfredsen et al., 2018), and to study riverbed evolution (Lane et al., 2003; Javernick et al., 2014; Dietrich, 2016; Cook, 2017). Recently, a further "grain" investigated in science has been underwater bathymetry reconstruction, with the pioneer works by Woodget et al. (2015, 2017) and Dietrich (2017). SfM photogrammetry in subaerial studies can provide consistent results if systematic errors due to refraction impact are accounted for (Mulsow et al., 2018). Partama et al. (2018) found that using coregistered image sequences or video frames to mitigate the

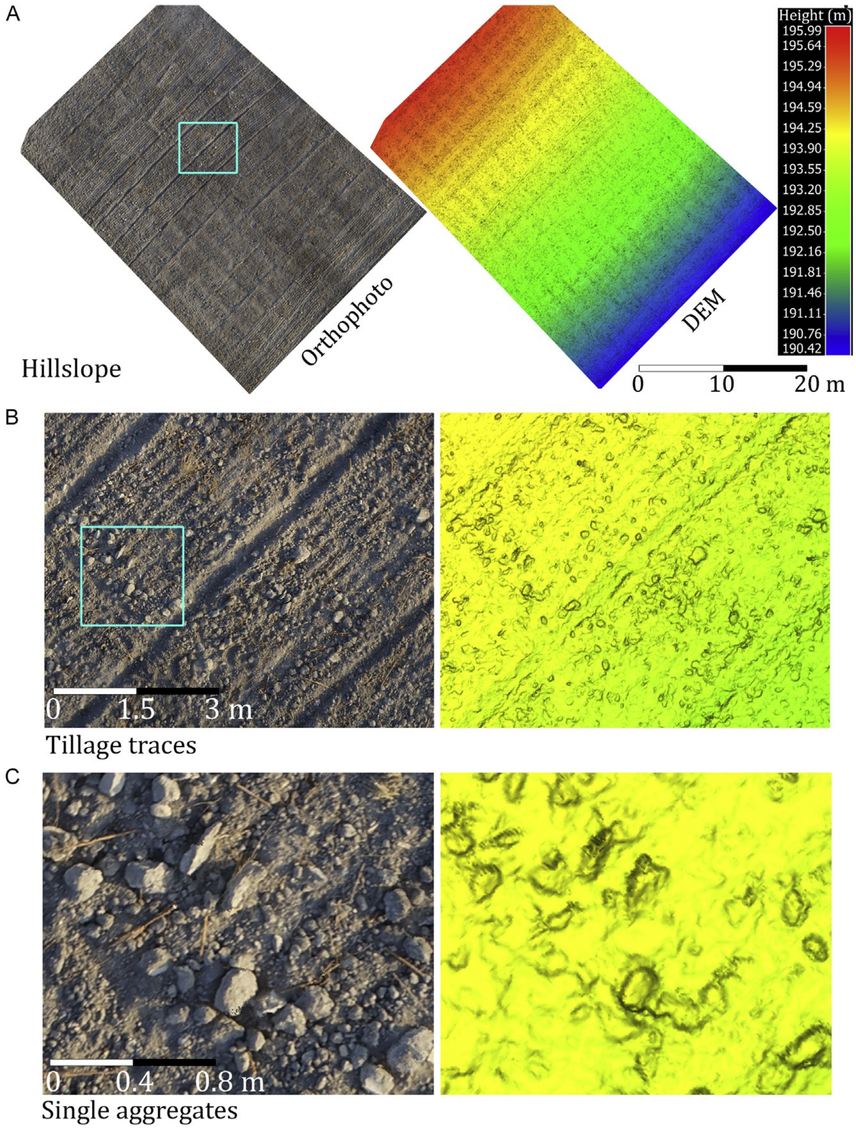

FIG. 3 Surface reconstruction across scales from UAV imagery (1 cm resolution) illustrated for a hillslope. (A) At hillslope scale, topographic features such as slope are measurable. (B) At the next scale traces for tillage (across-slope) and local potential accumulation spots become obvious. (C) At the last scale single aggregates, and, e.g., their relevance for roughness, can be evaluated.

effects of waves and water reflections could increase the size of reconstructed areas under difficult observation conditions. This method has the potential to significantly boost SfM-photogrammetry applications for bathymetric measurements. Overall, monitoring changes on stream channels with SfM photogrammetry gives a more complete spatial perspective than the traditional method of cross sections when quantifying small-scale geomorphic change.

Larger grains include gravitational processes, for example landslides, whose monitoring requires a continued assessment of the extent, the rate of displacement, surface topography, and detection of fissure structures that could be related to the processes. SfM photogrammetry in this field provides accurate, high-resolution topographic models that are fundamentally important for a detailed mapping both in mountain (Lucieer et al., 2014; Chidburee et al., 2016; Yu et al., 2017) or coastal environments (Genchi et al., 2015; Esposito et al., 2017a,b; Westoby et al., 2018). For these environments, SfM photogrammetry overcomes both the high economic costs of topographic data collection and the data-collection limits caused by the remoteness of field sites, which render other cheaper, portable surveying platforms (i.e., terrestrial laser scanning or GPS) impractical.

In addition, SfM photogrammetry has an advanced understanding of the dynamics of glaciers and rock glaciers (Piermattei et al., 2015; Ryan et al., 2015; Ely et al., 2017; Girod et al., 2017; Watson et al., 2017; Fugazza et al., 2018). Knowledge of changes in the extent, mass, and surface velocity of these grains contributes to a better understanding of the dynamic processes occurring in cold, high-mountain environments, and serves as an important contribution to climate monitoring.

4 Reconstructing processes in time

The high flexibility of SfM photogrammetry allows for repeated data acquisition and therefore multi-temporal earth surface observations with varying frequencies. In addition, the method can be applied to already existing image information enabling the reconstruction of past forms.

4.1 Past and real-time reconstruction

Recent works have highlighted the possibility of using archival photographs to reconstruct landscapes (Bakker and Lane, 2017), landscape processes and vegetation (Frankl et al., 2015; Gomez et al., 2015; Ishiguro et al., 2016), glaciers (Tonkin et al., 2016; Mertes et al., 2017; Midgley and Tonkin, 2017; Mölg and Bolch, 2017; Vargo et al., 2017), coastal changes (Warrick et al., 2017), and volcanic environments (Gomez, 2014; Gomez and Wassmer, 2015). In all these fields, the results provided a series of elevation models that demonstrated the potential for acquiring detailed and precise elevation data from any historical aerial imagery, provided, imagery is of the necessary scale to capture the features of interest. Reprocessing of these archives leads to point clouds with a significantly improved point density when processed with recently developed dense matching algorithms (Mölg and Bolch, 2017).

However, this literature also highlights the limitations of SfM photogrammetry applied to historical images. Whereas the ease of use gives SfM photogrammetry its major strength, the lack of transparency can make it difficult for non-specialist users to estimate the quality and accuracy of content derived from such materials (Brutto and Meli, 2012; Remondino et al., 2012), which is essential if workers are to evaluate the performance of 3D models derived from historical images. Furthermore, users need to consider that when analogue materials are digitized on nonphotogrammetric scanning platforms (Lane et al., 2010; Wheaton et al., 2010), nonsystematic geometric errors can be induced during the data-capture process, leading to subsequent problems when imagery is used in analytical applications (Verhoeven, 2011; Verhoeven et al., 2013; Sevara, 2016). The analysis of the evolution in 3D landforms based on historical images presents further difficulties because the pixel resolution of the early photographs is much lower than the recent ones. Volume and surface calculations must, therefore, be conducted carefully. Nevertheless, SfM-photogrammetry analysis can produce high-quality topographic datasets that are particularly useful in very active geomorphic areas, such as rivers, shores, glaciers, and volcanic environments, and when no, or only poor topographical data exists.

A further advance in SfM photogrammetry is currently offered by the availability of easily accessible rich imagery of large parts of the Earth's surface under many different viewing conditions, in terms of user-taken photographs or webcam services (Snavely et al., 2008, 2010; Sofia, 2020). This database of images presents enormous opportunities, both in research on computer vision and for practical applications in environmental research, especially for the reconstruction of extreme events (i.e., flash floods, landslides) for the purpose of rapidly obtaining critical "damage footprint" snapshots soon after the event. In the context of extreme events, for example, disaster-management systems such as the Copernicus Emergency Management Service (EMS) are currently not able to provide information products until up to 48–72 h after a disaster event has occurred, and planning topographic surveys requires time as well. In contrast, user-generated data such as social media posts or crowdsourced data are continuously produced and can be produced almost immediately because users actively participate throughout an event and share related information (Havas et al., 2017). This imagery has been considered only recently in the geosciences (Sylvest et al., 2014; Ratner et al., 2015; Haas et al., 2016; Raoult et al., 2016; Shaad et al., 2016; Guerin et al., 2017; Kobayashi et al., 2017; Sofia et al., 2017; Voumard et al., 2017; Chudý et al., 2018; Lewis and Park, 2018), but this type of application remains a major challenge for the scientific community.

One major drawback of internet-based or crowdsourced imagery is that these massive community photo collections are almost completely unstructured, making it difficult to use them for SfM applications (Snavely et al., 2010). Also, these photographs might not have been created specifically for documentation purposes, and so the focus of these images is generally not on the object to be evaluated. The image repositories must, therefore, be subjected to a preprocessing analysis of their photogrammetric usability. In many cases, with internet-based imagery, no reference information exists (e.g., GPS location of individual frames or GCPs at the area of interest). In addition, SfM-photogrammetry derived point clouds perform best with high-quality images, rather than from video frames or low-quality images (Westoby et al., 2012).

Despite these shortcomings, the above examples show how the resulting 3D models can be sufficiently detailed to permit basic analysis such as identification of features, or estimation of erosion volumes, for example. As an example, Fig. 4 shows the Oso landslide (WA) (Aaron et al., 2017; Stark et al., 2017), and a 3D reconstruction of the same landslide obtained using free software [VisualSFM and Meshlab] and a YouTube UAV-video (Martin, 2016) from which 200 frames have been obtained.

Challenges remain for the integration of this type of topography with 3D modeling, especially in the context of scaling of these technologies to provide coverage for larger areas. Data collection is commonly the most expensive and arduous task in many scientific disciplines, particularly those that involve fieldwork. This literature demonstrates that even without an extensive, time-consuming search, many images suitable for extracting scientific data already exist from crowdsourcing or internet-based services. Furthermore, internet searches can be both focused and guided if a clear path to obtaining the imagery exists. Although the estimated data might not be as accurate as a surveying campaign, the process could be simpler, faster, and less expensive, particularly if the areas are difficult to access.

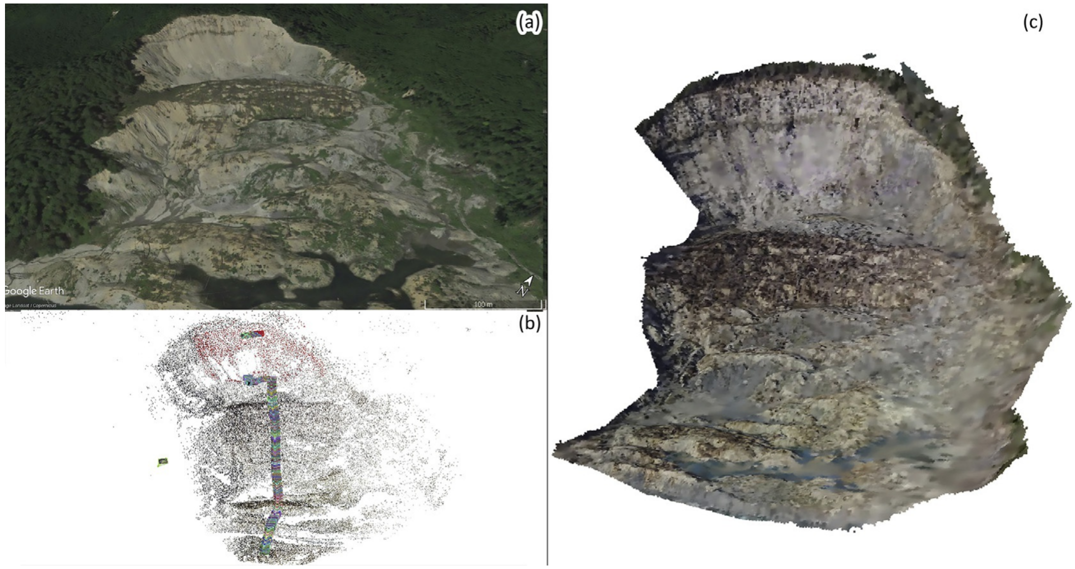

FIG. 4 3D reconstruction of the Oso landslide (WA). (A) Google Earth view (Map data: Google, LandSat/Copernicus) of the landslide; (B) point-cloud processed in VisualSFM and aligned video frames; (C) mesh reconstruction in MeshLab with a texture based on the RGB colors of the point cloud.

4.2 Time-lapse imagery for 4D change detection

The application of time-lapse imagery from multiple perspectives to perform 4D change detection has great potential for geomorphological studies because geomorphic processes might be observed in real-time. For TLS, time series of point clouds have already been utilized to observe rockfalls (Williams et al., 2018) and landslides (Kromer et al., 2017) with temporal resolutions of 1 h for a duration 10 months and 30 min for 6 weeks, respectively. However, in the field of image-based approaches, case studies are still limited. The available literature has highlighted examples related to lava flows (James and Robson, 2014), geological experiments in the laboratory (Galland et al., 2016), soil erosion (Eltner et al., 2017), and glacier ice-margin dynamics (Mallalieu et al., 2017). For these examples, the time resolution has varied from 1 to 10 min, and the timeframe of analysis ranges from $<$1 h (James and Robson, 2014) to 90 min (Eltner et al., 2017) to over 1 year (Mallalieu et al., 2017). This type of analysis is possible with different numbers of cameras [$<$5 cameras (Eltner et al., 2017; James and Robson, 2014), up to 15 (Mallalieu et al., 2017)] and results in very high precision datasets [0.1 mm (Galland et al., 2016) up to $>$10 mm (Eltner et al., 2017)].

4.2.1 Guidelines for time-lapse SfM photogrammetry

Several requirements and constraints limit the application of time-lapse SfM photogrammetry, which we list below. These constraints have thus far limited widespread adoption of the technique, but laboratory studies, where external parameters can be more easily constrained, demonstrate its enormous potential. The requirements and constraints of time-lapse SfM photogrammetry are:

- The interior camera geometry of the time-lapse cameras must be considered. Although Galland et al. (2016) were able to perform self-calibration in their study under presumably stable light conditions in the laboratory and very high overlap due to the close-range application, Eltner et al. (2017) performed camera calibration for each camera after the experiments. Due to less convergence and thus overlap of the images and due to changing luminance conditions, potential less measurement redundancy (observations from solely three cameras) caused less reliable estimation of camera parameters. This can lead to errors in the surface models, else might be mitigated with a fixed and pre-calibrated interior geometry. Another potential solution might be the implementation of a significantly higher number of cameras observing the same area. Also, Mallalieu et al. (2017) performed precamera calibration for their long-term observation. However, another issue comes into play that needs consideration: temporal stability of the interior geometry, especially due to strong changing temperatures over the year.
- Camera synchronization is another important issue if rapid changes are to be observed. Interior camera clocks or real-time clocks (RTC) can be used for synchronized triggering. But Mallalieu et al. (2017) measured a temporal drift of up to 30 min during long-term observations. Possible approaches for synchronization with subsecond accuracy is the use of a wired solution or applying radio transmission. However, the former method limits the distance between cameras, which might be unfavorable for large-range applications, and the latter method entails the risk of random failure of signal transmission. Another possibility is the use of GPS time, which is very precise but needs a higher power supply.
- Time-lapse imagery leads to a vast amount of images that need to be processed for each time interval. Thus, automation of the processing workflow is a requirement for sufficient data handling, among other prerequisites. Furthermore, the tool used to perform SfM photogrammetry must allow for script control of data processing, such as the python interface of PhotoScan (as illustrated by Eltner et al., 2017), or for general open-access options for programming, as it is the case with MicMac (as illustrated by Galland et al., 2016). For multitemporal change detection and analysis, the resulting point clouds need automated processing, as well.
- Application of time-lapse SfM photogrammetry in the field requires information about environmental conditions such as sun path, local topography, and prevailing weather conditions: these have impacts on image quality due to shadows, glare, and high-contrast images (Mallalieu et al., 2017). Furthermore, temporally stable GCPs are needed to capture changes of the intrinsic, as well as extrinsic camera parameters (e.g., Schwalbe and Maas, 2017). If the region of interest is at a larger distance, other targets than artificial GCPs are necessary due to the limited maximal size of GCPs. For instance, Mallalieu et al. (2017) and James et al. (2016) use natural features in the landscape to orient the cameras. However, their disadvantage is generally lower contrast and thus less precise data registration because measurements with sub-pixel accuracy, which can be obtained using artificial GCPs, are not possible. The introduction of time-SIFT by Feurer and Vinatier (2018) to automatically estimate cameras of multitemporal datasets in a single bundle adjustment, mainly relying on image observations, might be a future approach to deal with unstable camera geometries. In field applications, camera positions are mostly restricted by the topography and thus area access. However, if possible, the camera network geometry should be realized with convergent, high overlapping imagery, and sufficient perspective changes. Field-testing of the 3D reconstruction from the chosen camera positions is advised

prior cameras are permanently installed to ensure their placement is sufficient for a high-quality 3D model. Finally, for long-term observations, the cameras need sufficient power supplies, and the camera system has to be robust enough to withstand the environmental conditions at the field site. Ensuring the camera network is robust could potentially require the placement of redundant cameras to compensate for potential failure (Mallalieu et al., 2017).

5 Final remarks

Recent technological advances are revolutionizing geomorphology (Viles, 2016). Among them, image-based surface reconstruction using SFM is an established method: many case studies have demonstrated its suitability and performance across various spatiotemporal scales. Thus, in the future, the focus should be on retrieving geomorphological information to help understand forms and processes from (potentially still to develop) SfM derivatives.

Methodological advances are expected in the field of geo-referencing to further increase the flexibility of (multitemporal) topographic data retrieval. Increasing temporal resolution at unprecedented scales is also expected due to advances in the area of time-lapse photogrammetry. Furthermore, workflows for adequate deployment of preexisting and freely available large image repositories for geomorphic studies is another field for progress. Awareness regarding rigorous error estimation and parameter choices to improve models remains another important aspect for future applications.

SfM photogrammetry is a flexible, low-cost, and easy-to-use technique widely applied in the geosciences beyond the field of geomorphology because it enables democratic participation in research. Therefore, future studies should consider implementing this technique, including a sufficient understanding of the approach and suitable guidance to enable a fast involvement of end-users and researchers.

References

Aaron, J., Hungr, O., Stark, T.D., Baghdady, A.K., 2017. Oso, Washington, landslide of March 22, 2014: dynamic analysis. J. Geotech. Geoenviron. Eng. 143 (9).

Abellán, A., Jaboyedoff, M., Oppikofer, T., Vilaplana, J.M., 2009. Detection of millimetric deformation using a terrestrial laser scanner: experiment and application to a rockfall event. Nat. Hazards Earth Syst. Sci. 9 (2), 365–372.

AgiSoft LLC, 2010. AgiSoft PhotoScan Professional Edition.

Alfredsen, K., Haas, C., Tuhtan, J.A., Zinke, P., 2018. Brief communication: mapping river ice using drones and structure from motion. Cryosphere 12, 627–633.

Bakker, M., Lane, S.N., 2017. Archival photogrammetric analysis of river-floodplain systems using structure from motion (SfM) methods. Earth Surf. Process. Landf. 42 (8), 1274–1286.

Balaguer-Puig, M., Marqués-Mateu, Á., Lerma, J.L., Ibáñez-Asensio, S., 2017a. Estimation of small-scale soil erosion in laboratory experiments with structure from motion photogrammetry. Geomorphology 295, 285–296.

Balaguer-Puig, M., Marqués-Mateu, Á., Lerma, J.L., Sara Ibáñez-Asensio, S., 2017b. Quantifying small-magnitude soil erosion: geomorphic change detection at plot scale. Land Degrad. Dev. 29 (3), 825–834.

Benassi, F., Dall'Asta, E., Diotri, F., Forlani, G., di Cella, U.M., Roncella, R., Santise, M., 2017. Testing accuracy and repeatability of UAV blocks oriented with gnss-supported aerial triangulation. Remote Sens. (Basel) 9 (2), 1–23.

Bertin, S., Friedrich, H., 2016. Field application of close-range digital photogrammetry (CRDP) for grain-scale fluvial morphology studies. Earth Surf. Process. Landf. 41 (10), 1358–1369.

Bláha, M., Eisenbeiss, H., Grimm, D., Limpach, P., 2012. Direct georeferencing of Uavs. ISPRS Int. Arch. Photogramm. Remote Sens. Spatial Inf. Sci. XXXVIII(1C22), 131–136.

Bolles, R.C., Baker, H.H., Marimont, D.H., 1987. Epipolar-plane image analysis: an approach to determining structure from motion. Int. J. Comput. Vis. 1 (1), 7–55.

Brutto, M.L., Meli, P., 2012. Computer vision tools for 3D modelling in archaeology. Int. J. Herit. Digit. Era 1, 1–6.

Carbonneau, P.E., Dietrich, J.T., 2017. Cost-effective non-metric photogrammetry from consumer-grade sUAS: implications for direct georeferencing of structure from motion photogrammetry. Earth Surf. Process. Landf. 42 (3), 473–486.

Carrivick, J.L., Smith, M.W., Quincey, D.J., 2016. Structure from Motion in the Geosciences. Wiley-Blackwell.

Castillo, C., James, M.R., Redel-Macías, M.D., Pérez, R., Gómez, J.A., 2015. SF3M software: 3-D photo-reconstruction for non-expert users and its application to a gully network. Soil 1 (2), 583–594.

Chiang, K.W., Tsai, M.L., Chu, C.H., 2012. The development of an UAV borne direct georeferenced photogrammetric platform for ground control point free applications. Sensors 12 (7), 9161–9180.

Chidburee, P., Mills, J.P., Miller, P.E., Fieber, K.D., 2016. Towards a low-cost, real-time photogrammetric landslide monitoring system utilising mobile and cloud computing technology. ISPRS Int. Arch. Photogramm. Remote Sens. Spatial Inf. Sci. XLI(B5), 791–797.

Chudý, F., Slámová, M., Tomaštík, J., Tunák, D., Kardoš, M., Saloň, Š., 2018. The application of civic technologies in a field survey of landslides. Land Degrad. Dev. 29 (6), 1858–1870.

Cignoni, P., Callieri, M., Corsini, M., Dellepiane, M., Ganovelli, F., Ranzuglia, G., 2008. MeshLab: an open-source mesh processing tool. In: Scarano, V., De Chiara, R., Erra, U. (Eds.), Eurographics Italian Chapter Conference. The Eurographics Association.

Cook, K.L., 2017. An evaluation of the effectiveness of low-cost UAVs and structure from motion for geomorphic change detection. Geomorphology 278, 195–208.

Cramer, M., Stallmann, D., Haala, N., 2000. Direct georeferencing using gps/inertial exterior orientations for photogrammetric applications. ISPRS Int. Arch. Photogramm. Remote Sens. 33(B3), 198–205.

Dietrich, J.T., 2016. Riverscape mapping with helicopter-based structure-from-motion photogrammetry. Geomorphology 252, 144–157.

Dietrich, J.T., 2017. Bathymetric structure-from-motion: extracting shallow stream bathymetry from multi-view stereo photogrammetry. Earth Surf. Process. Landf. 42 (2), 355–364.

Eling, C., Wieland, M., Hess, C., Klingbeil, L., Kuhlmann, H., 2015. Development and evaluation of a uav based mapping system for remote sensing and surveying applications. ISPRS Int. Arch. Photogramm. Remote Sens. Spatial Inf. Sci. 40(1W4), 233–239.

Eltner, A., Schneider, D., 2015. Analysis of different methods for 3D reconstruction of natural surfaces from parallel-axes UAV images. Photogramm. Rec. 30 (151), 279–299.

Eltner, A., Kaiser, A., Castillo, C., Rock, G., Neugirg, F., Abellan, A., 2016. Image-based surface reconstruction in geomorphometry—merits, limits and developments. Earth Surf. Dyn. 4, 359–389.

Eltner, A., Kaiser, A., Abellan, A., Schindewolf, M., 2017. Time lapse structure from motion photogrammetry for continuous geomorphic monitoring. Earth Surf. Process. Landf. 42 (14), 2240–2253.

Eltner, A., Maas, H.-G., Faust, D., 2018. Soil micro-topography change detection at hillslopes in fragile Mediterranean landscapes. Geoderma. 313.

Ely, J.C., Graham, C., Barr, I.D., Rea, B.R., Spagnolo, M., Evans, J., 2017. Using UAV acquired photography and structure from motion techniques for studying glacier landforms: application to the glacial flutes at Isfallsglaciären. Earth Surf. Process. Landf. 42 (6), 877–888.

Entwistle, N., Heritage, G., Milan, D., 2018. Recent remote sensing applications for hydro and morphodynamic monitoring and modelling. Earth Surf. Process. Landf. 43 (10), 2283–2291.

Esposito, G., Mastrorocco, G., Salvini, R., Oliveti, M., Starita, P., 2017a. Application of UAV photogrammetry for the multi-temporal estimation of surface extent and volumetric excavation in the Sa Pigada Bianca open-pit mine, Sardinia, Italy. Environ. Earth Sci. 76.

Esposito, G., Salvini, R., Matano, F., Sacchi, M., Danzi, M., Somma, R., Troise, C., 2017b. Multitemporal monitoring of a coastal landslide through SfM-derived point cloud comparison. Photogramm. Rec. 32 (160), 459–479.

Feurer, D., Vinatier, F., 2018. Joining multi-epoch archival aerial images in a single SfM block allows 3-D change detection with almost exclusively image information. ISPRS J. Photogramm. Remote Sens. 146, 495–506.

Forlani, G., Dall'Asta, E., Diotri, F., di Cella, U.M., Roncella, R., Santise, M., 2018. Quality assessment of DSMs produced from UAV flights georeferenced with on-board RTK positioning. Remote Sens. (Basel) 10 (2), 311.

Frankl, A., Seghers, V., Stal, C., De Maeyer, P., Petrie, G., Nyssen, J., 2015. Using image-based modelling (SfM–MVS) to produce a 1935 ortho-mosaic of the Ethiopian highlands. Int. J. Digit. Earth 8 (5), 421–430.

Fugazza, D., Scaioni, M., Corti, M., D'agata, C., Azzoni, R.S., Cernuschi, M., … Diolaiuti, G.A., 2018. Combination of UAV and terrestrial photogrammetry to assess rapid glacier evolution and map glacier hazards. Hazards Earth Syst. Sci. *18*, 1055–1071.

Gabrlik, P., la Cour-Harbo, A., Kalvodova, P., Zalud, L., Janata, P., 2018. Calibration and accuracy assessment in a direct georeferencing system for UAS photogrammetry. Int. J. Remote Sens. 39, 4931–4959.

Galland, O., Bertelsen, H.S., Guldstrand, F., Girod, L., Johannessen, R.F., Bjugger, F., … Mair, K., 2016. Application of open-source photogrammetric software MicMac for monitoring surface deformation in laboratory models. J. Geophys. Res. Solid Earth 121 (4), 2852–2872.

Genchi, S.A., Vitale, A.J., Perillo, G.M.E., Delrieux, C.A., 2015. Structure-from-motion approach for characterization of bioerosion patterns using UAV imagery. Sensors 15, 3593–3609.

Gerke, M., Przybilla, H.-J., 2016. Accuracy analysis of photogrammetric UAV image blocks: influence of onboard RTK-GNSS and cross flight patterns. Photogramm. Fernerkundung Geoinf. 2016 (1), 17–30.

Gessesse, G.D., Fuchs, H., Mansberger, R., Klik, A., Rieke-Zapp, D.H., 2010. Assessment of erosion, deposition and rill development on irregular soil surfaces using close range digital photogrammetry. Photogramm. Rec. 25 (131), 299–318.

Girardeau-Montaut, D. (2015). CloudCompare (version 2.7) [GPL software]. (2015). Retrieved from http://www.cloudcompare.org/. Telecom ParisTechParis.

Girod, L., Nuth, C., Kääb, A., Etzelmüller, B., Kohler, J., 2017. Terrain changes from images acquired on opportunistic flights by SfM photogrammetry. Cryosphere 11 (2), 827–840.

Glendell, M., McShane, G., Farrow, L., James, M.R., Quinton, J., Anderson, K., Evans, M., Benaud, P., Rawlins, B., Morgan, D., Jones, L., Kirkham, M., DeBell, L., Quine, T., Lark, M., Rickson, J., Brazier, R.E., 2017. Testing the utility of structure from motion photogrammetry reconstructions using small unmanned aerial vehicles and ground photography to estimate the extent of upland soil erosion. Earth Surf. Process. Landf. 42 (12), 1860–1871.

Goetz, J., Brenning, A., Marcer, M., Bodin, X., 2018. Modeling the precision of structure-from-motion multi-view stereo digital elevation models from repeated close-range aerial surveys. Remote Sens. Environ. 210, 208–216.

Gomez, C., 2014. Digital photogrammetry and GIS-based analysis of the bio-geomorphological evolution of Sakurajima volcano, diachronic analysis from 1947 to 2006. J. Volcanol. Geotherm. Res. 280, 1–13.

Gomez, C., Wassmer, P., 2015. Evolution of the Unzen volcano and the Shimabara Peninsula (Japan) during the last 60 years: the role of the 1990-1995 eruption in modifying the landscape. Géomorphol. Relief Process. Environ. 21 (3), 205–216.

Gomez, C., Hayakawa, Y., Obanawa, H., 2015. A study of Japanese landscapes using structure from motion derived DSMs and DEMs based on historical aerial photographs: new opportunities for vegetation monitoring and diachronic geomorphology. Geomorphology 242, 11–20.

Gruen, A., 2012. Development and status of image matching in photogrammetry. Photogramm. Rec. 27 (137), 36–57.

Guerin, A., Abellán, A., Matasci, B., Jaboyedoff, M., Derron, M.H., Ravanel, L., 2017. Brief communication: 3-D reconstruction of a collapsed rock pillar from web-retrieved images and terrestrial lidar data-the 2005 event of the west face of the Drus (Mont Blanc massif). Nat. Hazards Earth Syst. Sci. 17 (7), 1207–1220.

Haas, F., Wegner, K., Mangeney, A., Durand, V., 2016. Detection of rock failures in the Dolomieu crater on La Réunion using multitemporal LiDAR and photogrammetric data. Geophys. Res. Abstr. 18, EGU2016-17112.

Hänsel, P., Schindewolf, M., Eltner, A., Kaiser, A., Schmidt, J., 2016. Feasibility of high-resolution soil erosion measurements by means of rainfall simulations and SfM photogrammetry. Hydrology 3, 38.

Havas, C., Resch, B., Francalanci, C., Pernici, B., Scalia, G., Fernandez-Marquez, J.L., Van Achte, T., Zeug, G., Mondardini, M.R.R., Grandoni, D., Kirsch, B., Kalas, M., Lorini, V., Rüping, S., 2017. E2mC: improving emergency management service practice through social media and crowdsourcing analysis in near real time. Sensors 17(12).

Heimsath, A.M., Farid, H., 2002. Hillslope topography from unconstrained photographs. Math. Geol. 34 (8), 929–952.

Hemmelder, S., Marra, W., Markies, H., De Jong, S.M., 2018. Monitoring river morphology & bank erosion using UAV imagery—a case study of the river Buëch, Hautes-Alpes, France. Int. J. Appl. Earth Observ. Geoinf. 73, 428–437.

Hugenholtz, C., Brown, O., Walker, J., Barchyn, T., Nesbit, P., Kucharczyk, M., Myshak, S., 2016. Spatial accuracy of UAV-derived orthoimagery and topography: comparing photogrammetric models processed with direct georeferencing and ground control points. Geomatica 70, 21–30.

Ishiguro, S., Yamano, H., Oguma, H., 2016. Evaluation of DSMs generated from multi-temporal aerial photographs using emerging structure from motion-multi-view stereo technology. Geomorphology 268, 64–71.

James, M.R., Robson, S., 2012. Straightforward reconstruction of 3D surfaces and topography with a camera: accuracy and geoscience application. J. Geophys. Res. 117.
James, M., Robson, S., 2014. Mitigating systematic error in topographic models derived from UAV and ground-based image networks. Earth Surface Process. Landf. 39 (10), 1413–1420.
James, M.R., How, P., Wynn, P.M., 2016. Pointcatcher software: analysis of glacial time-lapse photography and integration with multitemporal digital elevation models. J. Glaciol. 62 (231), 159–169.
James, M.R., Robson, S., d'Oleire-Oltmanns, S., Niethammer, U., 2017a. Optimising UAV topographic surveys processed with structure-from-motion: ground control quality, quantity and bundle adjustment. Geomorphology 280, 51–66.
James, M.R., Robson, S., Smith, M.W., 2017b. 3-D uncertainty-based topographic change detection with structure-from-motion photogrammetry: precision maps for ground control and directly georeferenced surveys. Earth Surf. Process. Landf. 42 (12), 1769–1788.
James, M., Chandler, J., Eltner, A., Fraser, C., Miller, P., Mills, J., Noble, T., Robson, S., Lane, S., 2019. Guidelines on the use of structure from motion photogrammetry in geomorphic research. Earth Surface Process. Landf. 44, 2081–2084.
Javernick, L., Brasington, J., Caruso, B., 2014. Modeling the topography of shallow braided rivers using structure-from-motion photogrammetry. Geomorphology 213, 166–182.
Jugie, M., Gob, F., Virmoux, C., Brunstein, D., Tamisier, V., Le Coeur, C., Grancher, D., 2018. Characterizing and quantifying the discontinuous bank erosion of a small low energy river using structure-from-motion photogrammetry and erosion pins. J. Hydrol. 563, 418–434.
Kaiser, A., Erhardt, A., Eltner, A., 2018. Addressing uncertainties in interpreting soil surface changes by multitemporal high-resolution topography data across scales. Land Degrad. Dev. 29 (8), 2264–2277.
Kobayashi, K., Shishido, H., Kameda, Y., Kitahara, I., 2017. Method to generate disaster-damage map using 3D photometry and crowd sourcing. In: IEEE International Conference on Big Data (Big Data), pp. 4397–4399.
Kröhnert, M., Anderson, R., Bumberger, J., Dietrich, P., Harpole, W., Maas, H.-G., 2018. Watching grass grow—a pilot study on the suitability of photogrammetric techniques for quantifying change in aboveground biomass in grassland experiments. ISPRS Int. Arch. Photogramm. Remote Sens. Spatial Inf. Sci. XLII, 4–7.
Kromer, R., Abellán, A., Hutchinson, D., Lato, M., Edwards, T., Jaboyedoff, M., 2015. A 4D filtering and calibration technique for small-scale point cloud change detection with a terrestrial laser scanner. Remote Sens. (Basel) 7 (10), 13029–13052.
Kromer, R.A., Abellán, A., Hutchinson, D.J., Lato, M., Chanut, M.-A., Dubois, L., Jaboyedoff, M., 2017. Automated terrestrial laser scanning with near-real-time change detection—monitoring of the Séchilienne landslide. Earth Surf. Dyn. 5, 293–310. https://doi.org/10.5194/esurf-5-293-2017.
Lague, D., Brodu, N., Leroux, J., 2013. Accurate 3D comparison of complex topography with terrestrial laser scanner: application to the Rangitikei canyon (N-Z). ISPRS J. Photogramm. Remote Sens. 82, 10–26.
Lane, S.N., Westaway, R.M., Murray Hicks, D., 2003. Estimation of erosion and deposition volumes in a large, gravel-bed, braided river using synoptic remote sensing. Earth Surf. Process. Landf. 28, 249–271.
Lane, S.N., Widdison, P.E., Thomas, R.E., Ashworth, P.J., Best, J.L., Lunt, I.A., … Simpson, C.J., 2010. Quantification of braided river channel change using archival digital image analysis. Earth Surf. Process. Landf. 35 (8), 971–985.
Lewis, Q.W., Park, E., 2018. Volunteered geographic videos in physical geography: data mining from YouTube. Ann. Am. Assoc. Geogr. 108 (1), 52–70.
Lowe, D.G., 2004. Distinctive image features from scale-invariant keypoints. Int. J. Comput. Vis. 60 (2), 91–110.
Lucieer, A., de Jong, S.M., Turner, D., 2014. Mapping landslide displacements using structure from motion (SfM) and image correlation of multi-temporal UAV photography. Progr. Phys. Geogr. 38 (1), 97–116.
Mallalieu, J., Carrivick, J.L., Quincey, D.J., Smith, M.W., James, W.H.M., 2017. An integrated structure-from-motion and time-lapse technique for quantifying ice-margin dynamics. J. Glaciol. 63 (242), 937–949.
Mancini, F., Dubbini, M., Gattelli, M., Stecchi, F., Fabbri, S., Gabbianelli, G., 2013. Using unmanned aerial vehicles (UAV) for high-resolution reconstruction of topography: the structure from motion approach on coastal environments. Remote Sens. (Basel) 5, 6880–6898.
Marr, D., Poggio, T., 1976. Cooperative computation of stereo disparity. Science 194 (4262), 283–287.
Marteau, B., Vericat, D., Gibbins, C., Batalla, R.J., Green, D.R., 2017. Application of structure-from-motion photogrammetry to river restoration. Earth Surf. Process. Landf. 42 (3), 503–515.
Martin, M., 2016. OSO Washington Landslide Aerial Footage Inspire 1 (Drone). YouTube.

Maybank, S., 1993. Theory of Reconstruction From Image Motion. Springer, Berlin Heidelberg.
Mertes, J.R., Gulley, J.D., Benn, D.I., Thompson, S.S., Nicholson, L.I., 2017. Using structure-from-motion to create glacier DEMs and orthoimagery from historical terrestrial and oblique aerial imagery. Earth Surf. Process. Landf. 42 (14), 2350–2364.
Mian, O., Lutes, J., Lipa, G., Hutton, J.J., Gavelle, E., Borghini, S., 2015. Direct georeferencing on small unmanned aerial platforms for improved reliability and accuracy of mapping without the need for ground control points. ISPRS Int. Arch. Photogramm. Remote Sens. Spatial Inf. Sci. 40(1W4), 397–402.
Micheletti, N., Chandler, J.H., Lane, S.N., 2014. Investigating the geomorphological potential of freely available and accessible structure-from-motion photogrammetry using a smartphone. Earth Surf. Process. Landf. 40, 473–486.
Midgley, N.G., Tonkin, T.N., 2017. Reconstruction of former glacier surface topography from archive oblique aerial images. Geomorphology 282, 18–26.
Miller, H.J., Goodchild, M.F., 2015. Data-driven geography. GeoJournal 80 (4), 449–461.
Mölg, N., Bolch, T., 2017. Structure-from-motion using historical aerial images to analyse changes in glacier surface elevation. Remote Sens. (Basel) 9(10).
Morgan, J.A., Brogan, D.J., Nelson, P.A., 2017. Application of structure-from-motion photogrammetry in laboratory flumes. Geomorphology 276, 125–143.
Mosbrucker, A.R., Major, J.J., Spicer, K.R., Pitlick, J., 2017. Camera system considerations for geomorphic applications of SfM photogrammetry. Earth Surf. Process. Landf. 42 (6), 969–986.
Mulsow, C., Kenner, R., Bühler, Y., Stoffel, A., Maas, H.-G., 2018. Subaquatic digital elevation models from UAV-imagery. ISPRS Int. Arch. Photogramm. Remote Sens. Spatial Inf. Sci. XLII(2), 739–744.
Nouwakpo, S.K., Weltz, M.A., McGwire, K., 2015. Assessing the performance of structure-from-motion photogrammetry and terrestrial lidar for reconstructing soil surface microtopography of naturally vegetated plots. Earth Surf. Process. Landf. 41 (3), 308–322.
O'Connor, J., Smith, M.J., James, M.R., 2017. Cameras and settings for aerial surveys in the geosciences: optimising image data. Progr. Phys. Geogr. 41 (3), 325–344.
Partama, I.G.Y., Kanno, A., Ueda, M., Akamatsu, Y., Inui, R., Sekine, M., Yamamoto, K., Imai, T., Higuchi, T., 2018. Removal of water-surface reflection effects with a temporal minimum filter for UAV-based shallow-water photogrammetry. Earth Surf. Process. Landf. 43 (12), 2673–2682.
Pearson, E., Smith, M.W., Klaar, M.J., Brown, L.E., 2017. Can high resolution 3D topographic surveys provide reliable grain size estimates in gravel bed rivers? Geomorphology 293, 143–155.
Pfeifer, N., Glira, P., Briese, C., 2012. Direct georeferencing with on board navigation components of light weight Uav platforms. ISPRS Int. Arch. Photogramm. Remote Sens. Spatial Inf. Sci. XXXIX(B7), 487–492.
Piermattei, L., Carturan, L., de Blasi, F., Tarolli, P., Dalla Fontana, G., Vettore, A., Pfeifer, N., 2015. Analysis of glacial and periglacial processes using structure from motion. Earth Surf. Dyn. Discuss. 3 (4), 1345–1398.
Pierrot-Deseilligny, M., Clery, I., 2011. APERO, an open source bundle adjustment software for automatic calibration and orientation of set of images. Int. Arch. Photogramm. Remote Sens. Spatial Inf. Sci. 38–5 (W16), 269–276.
Prosdocimi, M., Calligaro, S., Sofia, G., Dalla Fontana, G., Tarolli, P., 2016. Bank erosion in agricultural drainage networks: new challenges from structure-from-motion photogrammetry for post-event analysis. Earth Surf. Process. Landf. 40, 1891–1906.
Prosdocimi, M., Burguet, M., Di Prima, S., Sofia, G., Terol, E., Rodrigo Comino, J., Cerdà, A., Tarolli, P., 2017. Rainfall simulation and structure-from-motion photogrammetry for the analysis of soil water erosion in Mediterranean vineyards. Sci. Total Environ. 574, 204–215.
Raoult, V., David, P.A., Dupont, S.F., Mathewson, C.P., O'Neill, S.J., Powell, N.N., Williamson, J.E., 2016. GoPros™ as an underwater photogrammetry tool for citizen science. PeerJ. 4.
Ratner, J., Pyle, D., Mather, T., 2015. Investigating the effects of methodological expertise and data randomness on the robustness of crowd-sourced SfM terrain models. Geophys. Res. Abstr. 17, EGU2015-6676.
Rehak, M., Skaloud, J., 2016. Applicability of new approaches of sensor orientation to micro aerial vehicles. ISPRS Ann. Photogramm. Remote Sens. Spatial Inf. Sci. III(3), 441–447.
Rehak, M., Mabillard, R., Skaloud, J., 2013. A micro-UAV with the capability of direct georeferencing. ISPRS Int. Arch. Photogramm. Remote Sens. Spatial Inf. Sci. XL(1W2), 317–323.
Remondino, F., Del Pizzo, S., Kersten, T.P., Troisi, S., 2012. Low-cost and open-source solutions for automated image orientation—a critical overview. Progr. Cult. Herit. Preserv. 44–54. EuroMed 2012.
Remondino, F., Spera, M.G., Nocerino, E., Menna, F., Nex, F., 2014. State of the art in high density image matching. Photogramm. Rec. 29 (146), 144–166.

Remondino, F., Nocerino, E., Toschi, I., Menna, F., 2017. A critical review of automated photogrammetric processing of large datasets. ISPRS Int. Arch. Photogramm. Remote Sens. Spatial Inf. Sci. XLII(2/W5), 591–599.

Rosnell, T., Honkavaara, E., 2012. Point cloud generation from aerial image data acquired by a quadrocopter type micro unmanned aerial vehicle and a digital still camera. Sensors 12, 453–480.

Ryan, J.C., Hubbard, A.L., Box, J.E., Todd, J., Christoffersen, P., Carr, J.R., Holt, T., Snooke, N., 2015. UAV photogrammetry and structure from motion to assess calving dynamics at store glacier, a large outlet draining the Greenland ice sheet. Cryosphere 9 (1), 1–11.

Schonberger, J.L., Frahm, J.-M., 2016. Structure-from-motion revisited. In: IEEE Conference on Computer Vision and Pattern Recognition (CVPR), pp. 4104–4113.

Schwalbe, E., Maas, H.G., 2017. The determination of high-resolution spatio-temporal glacier motion fields from time-lapse sequences. Earth Surf. Dyn. 5 (4), 861–879.

Sevara, C., 2016. Capturing the past for the future: an evaluation of the effect of geometric scan deformities on the performance of aerial archival media in image-based modelling environments. Archaeol. Prospect. 23 (4), 325–334.

Shaad, K., Ninsalam, Y., Padawangi, R., Burlando, P., 2016. Towards high resolution and cost-effective terrain mapping for urban hydrodynamic modelling in densely settled river-corridors. Sustain. Cities Soc. 20, 168–179.

Slama, C.C., Theurer, C., Henriksen, S.W. (Eds.), 1980. Manual of Photogrammetry. American Society for Photogrammetry and Remote Sensing. American Society of Photogrammetry.

Smith, M.W., Vericat, D., 2015. From experimental plots to experimental landscapes: topography, erosion and deposition in sub-humid badlands from structure-from-motion photogrammetry. Earth Surf. Process. Landf. 40 (12), 1656–1671.

Smith, M.W., Warburton, J., 2018. Microtopography of bare peat: a conceptual model and objective classification from high-resolution topographic survey data. Earth Surf. Process. Landf. 43 (8), 1557–1574.

Smith, M.W., Carrivick, J.L., Quincey, D.J., 2016. Structure from motion photogrammetry in physical geography. Progr. Phys. Geogr. 40 (2), 247–275.

Snavely, N., Seitz, S.M., Szeliski, R., 2006. Photo tourism: exploring photo collections in 3D. ACM Trans. Graph. 25 (3), 835–846.

Snavely, N., Seitz, S.M., Szeliski, R., 2008. Modeling the world from internet photo collections. Int. J. Comput. Vis. 80 (2), 189–210.

Snavely, N., Simon, I., Goesele, M., Szeliski, R., Seitz, S.M., 2010. Scene reconstruction and visualization from community photo collections. Proc. IEEE 98 (8), 1370–1390.

Sofia, G., 2020. Combining geomorphometry, feature extraction techniques and Earth-surface processes research: the way forward. Geomorphology 355, 107055.

Sofia, G., Bailly, J.-S., Chehata, N., Tarolli, P., Levavasseur, F., 2016. Comparison of Pleiades and LiDAR digital elevation models for terraces detection in farmlands. IEEE J. Sel. Top. Appl. Earth Observ. Remote Sens. 9 (4), 1567–1576.

Sofia, G., Masin, R., Tarolli, P., 2017. Prospects for crowd sourced information on the geomorphic 'engineering' by the invasive Coypu (*Myocastor coypus*). Earth Surf. Process. Landf. 42 (2), 365–377.

Stark, T.D., Baghdady, A.K., Hungr, O., Aaron, J., 2017. Case study: Oso, Washington, landslide of march 22, 2014—material properties and failure mechanism. J. Geotech. Geoenviron. Eng. 143 (5).

Stöcker, C., Nex, F., Koeva, M., Gerke, M., 2017. Quality assessment of combined IMU/GNSS data for direct georeferencing in the context of UAV-based mapping. ISPRS Int. Arch. Photogramm. Remote Sens. Spatial Inf. Sci. XLII(2W6), 355–361.

Sylvest, M.E., Dixon, J.C., Leone, R.C., Barnes, A., 2014. DEM extraction from stereo webcam videos for small-scale experimental geomorphological modeling. Lunar Planet. Sci. Conf. 45.

Tarolli, P., Cavalli, M., Masin, R., 2019. High-resolution morphologic characterization of conservation agriculture. Catena 172, 846–856.

Tonkin, T.N., Midgley, N.G., 2016. Ground-control networks for image based surface reconstruction: an investigation of optimum survey designs using UAV derived imagery and structure-from-motion photogrammetry. Remote Sens. (Basel) 8 (9), 16–19.

Tonkin, T.N., Midgley, N.G., Cook, S.J., Graham, D.J., 2016. Ice-cored moraine degradation mapped and quantified using an unmanned aerial vehicle: a case study from a polythermal glacier in Svalbard. Geomorphology 258, 1–10.

Turner, D., Lucieer, A., Wallace, L., 2014. Direct georeferencing of ultrahigh-resolution UAV imagery. IEEE Trans. Geosci. Remote Sens. 52 (5), 2738–2745.

Ullman, S., 1979. The Interpretation of Visual Motion. MIT Press.

Vargo, L.J., Anderson, B.M., Horgan, H.J., Mackintosh, A.N., Lorrey, A.M., Thornton, M., 2017. Using structure from motion photogrammetry to measure past glacier changes from historic aerial photographs. J. Glaciol. 63 (242), 1105–1118.

Verhoeven, G., 2011. Taking computer vision aloft—archaeological three-dimensional reconstructions from aerial photographs with photoscan. Archaeol. Prospect. 18 (1), 67–73.

Verhoeven, G., Sevara, C., Karel, W., Ressl, C., Doneus, M., Briese, C., 2013. Undistorting the past: new techniques for orthorectification of archaeological aerial frame imagery. In: Corsi, C., Slapska, B., Vermeulen, F. (Eds.), Good Practice in Archaeological Diagnostics, pp. 31–67.

Viles, H., 2016. Technology and geomorphology: are improvements in data collection techniques transforming geomorphic science? Geomorphology 270, 121–133.

Voumard, J., Abellán, A., Nicolet, P., Penna, I., Chanut, M.A., Derron, M.H., Jaboyedoff, M., 2017. Using street view imagery for 3-D survey of rock slope failures. Nat. Hazards Earth Syst. Sci. 17 (12), 2093–2107.

Warrick, J.A., Ritchie, A.C., Adelman, G., Adelman, K., Limber, P.W., 2017. New techniques to measure cliff change from historical oblique aerial photographs and structure-from-motion photogrammetry. J. Coast. Res. 331 (1), 39–55.

Wasklewicz, T., Zhu, Z., Gares, P., 2017. Simulating and quantifying legacy topographic data uncertainty: an initial step to advancing topographic change analyses. Progr. Earth Planet. Sci. 4(1).

Watson, C.S., Quincey, D.J., Smith, M.W., Carrivick, J.L., Rowan, A.V., James, M.R., 2017. Quantifying ice cliff evolution with multi-temporal point clouds on the debris-covered Khumbu glacier, Nepal. J. Glaciol. 63 (241), 823–837.

Westoby, M.J.J., Brasington, J., Glasser, N.F.F., Hambrey, M.J.J., Reynolds, J.M.M., 2012. "Structure-from-motion" photogrammetry: a low-cost, effective tool for geoscience applications. Geomorphology 179, 300–314.

Westoby, M.J., Lim, M., Hogg, M., Pound, M.J., Dunlop, L., Woodward, J., 2018. Cost-effective erosion monitoring of coastal cliffs. Coast. Eng. 138, 152–164.

Wheaton, J.M., Brasington, J., Darby, S.E., Sear, D.A., 2010. Accounting for uncertainty in DEMs from repeat topographic surveys: improved sediment budgets. Earth Surf. Process. Landf. 35 (2), 136–156.

Williams, J.G., Rosser, N.J., Hardy, R.J., Brain, M.J., Afana, A.A., 2018. Optimising 4-D surface change detection: an approach for capturing rockfall magnitude–frequency. Earth Surf. Dyn. 6, 101–119. https://doi.org/10.5194/esurf-6-101-2018.

Woodget, A.S., Austrums, R., 2017. Subaerial gravel size measurement using topographic data derived from a UAV-SfM approach. Earth Surf. Process. Landf. 42 (9), 1434–1443.

Woodget, A.S., Carbonneau, P.E., Visser, F., Maddock, I.P., 2015. Quantifying submerged fluvial topography using hyperspatial resolution UAS imagery and structure from motion photogrammetry. Earth Surf. Process. Landf. 40 (1), 47–64.

Wu, C. (2011). Visual SFM: A visual structure from motion system. http://ccwu.me/vsfm, 9.

Wu, C., 2013. Towards linear-time incremental structure from motion. In: International Conference on 3D Vision—3DV, pp. 127–134.

Yu, M., Huang, Y., Zhou, J., Mao, L., 2017. Modeling of landslide topography based on micro-unmanned aerial vehicle photography and structure-from-motion. Environ. Earth Sci. 76 (15).

Zhu, R., Wang, C., Lin, C.-H., Wang, Z., Lucey, S., 2018. Object-centric photometric bundle adjustment with deep shape prior. In: IEEE Winter Conference on Applications of Computer Vision (WACV), pp. 894–902.

Further reading

Clapuyt, F., Vanacker, V., van Oost, K., Schlunegger, F., 2015. Very-high resolution monitoring of movement of surface material within a landslide. In: Jasiewicz, J., Zwoliński, Z., Mitasova, H., Hengl, T. (Eds.), Geomorphometry for Geosciences. pp. 185–188.

Furukawa, Y., Ponce, J., 2010. Accurate, dense, and robust multiview stereopsis. IEEE Trans. Pattern Anal. Mach. Intell. 83, 1362–1376.

Pikelj, K., Ružić, I., Ilić, S., James, M.R., Kordić, B., 2018. Implementing an efficient beach erosion monitoring system for coastal management in Croatia. Ocean Coast. Manag. 156, 223–238.

Woodget, A.S., Austrums, R., Maddock, I.P., Habit, E., 2017a. Drones and digital photogrammetry: from classifications to continuums for monitoring river habitat and hydromorphology. WIREs Water. 4(4).

Woodget, A.S., Fyffe, C., Carbonneau, P.E., 2017b. From manned to unmanned aircraft: adapting airborne particle size mapping methodologies to the characteristics of sUAS and SfM. Earth Surf. Process. Landf. 43 (4), 857–870.